Quantum discrete ϕ^4 model at finite temperatures

V. V. Savkin and A. N. Rubtsov
Physics Department, Moscow State University, 119899 Moscow, Russia

T. Janssen
Institute of Theoretical Physics, University of Nijmegen, Postbus 9010, 6500 GL Nijmegen, The Netherlands

(Received 13 December 2001; revised manuscript received 14 March 2002; published 21 May 2002)

Quantum phase transitions are studied in the framework of the quantum discrete ϕ^4 model at zero and finite temperatures by quantum Monte Carlo calculations and the simplest analytical approximations. Parameters of the model (mass m, temperature t, and dimensionless parameter a) allow us to go continuously from quantum ($t=0$) to classical ($m\to+\infty$) phase transitions and from displacive ($a\to+0$) to order-disorder ($a\to+\infty$) ones. Phase diagrams (dependencies of the critical mass on the critical temperature) are obtained for two- and three-dimensional systems for various values of the parameter a. The quantum Monte Carlo results show excellent agreement with previous studies of the discrete ϕ^4 model in the various limits. The obtained quantum Monte Carlo data are compared with results of the mean-field and independent-mode approaches. The mean-field approximation is in qualitative agreement with quantum Monte Carlo results for a wide range of the parameter a of the model, while the independent-mode one is in quantitative agreement at small values of a. The obtained results can be used for estimations of the behavior of real ferroelectrics.

DOI: 10.1103/PhysRevB.65.214103 PACS number(s): 64.60.Cn, 63.70.+h, 73.43.Nq

I. INTRODUCTION

Two types of fluctuations are present in real systems in the general case: thermal and quantum ones. Thermal fluctuations govern ordering in systems at high temperatures, while quantum effects are constitutive in the physical picture at low temperatures or at small masses. The situation when both types of fluctuations play an essential role is interesting. Normally, quantum fluctuations suppress phase transitions at low temperatures in various materials, leaving them in a disordered phase. Ferroelectrics are well-investigated materials showing this phenomenon. So-called quantum paraelectric materials ($SrTiO_3$, $BaTiO_3$, $KTaO_3$) are extensively studied both theoretically and experimentally. For example, the biquadratic ferroelectric mode-coupling theory predicted an intrinsic paraelectric quantum state of $SrTiO_3$.[1] Recently, the restoration of ferroelectricity in $SrTiO_3$ by changing oxygen O^{16} to the heavier isotope O^{18} was reported.[2] This effect was studied using a self-consistent phonon approximation in Ref. 3 for $SrTiO_3$ and $KTaO_3$ (other approaches concerning these materials are described in Ref. 4). $BaTiO_3$ as a high-temperature ferroelectric shows also a strong influence of quantum fluctuations as was shown in Ref. 5–7 by numerical calculations, in the framework of the Ising model in a transverse field and from first principles. The dielectric susceptibility in the frame of this approach as well as other properties were obtained in good agreement with experimental data for various ferroelectrics.[8–10]

Among structural phase transitions one may distinguish displacive and order-disorder types. Ferromagnetics usually reveal an order-disorder type of phase transition, while displacive transitions occur in ferroelectrics. However, there are ferroelectrics that show order-disorder (for example, KH_2PO_4) or neither displacive nor order-disorder behavior (for example, $Sn_2P_2S_6$).[11] A suitable and well-known microscopic model for this case is the discrete ϕ^4 model.[12] This model shows a continuous crossover from displacive phase transitions to the order-disorder ones. Quantum fluctuations can also be introduced into this model. Thus, this model can cover a wide class of materials that can reveal structural phase transitions with an influence of thermal and quantum effects. However, only limiting cases of this model were studied.

In this paper we study the general case of the quantum discrete ϕ^4 model in the presence of quantum and thermal fluctuations. We consider a simple cubic [three-dimensional (3D)] or square [two-dimensional (2D)] lattice of particles of mass M. The displacements of particles from equilibrium positions are determined by a scalar function X_n. We suppose that every atom is placed in a double-well potential with harmonic coupling with nearest neighbors. The Hamiltonian of the discrete ϕ^4 model is as follows:

$$H=\sum_n \frac{P_n^2}{2M}+V,$$

$$V=-\frac{A}{2}\sum_n X_n^2+\frac{B}{4}\sum_n X_n^4 + \frac{C}{2}\sum_{n,n'}(X_n-X_{n'})^2\sigma_{nn'}. \quad (1)$$

Here, $\sigma_{nn'}=1$ for nearest neighbors and vanishes elsewhere. A second-order phase transition takes place for positive values of A,B, and C if the dimensionality of the system d is larger than 1. Previous studies of this model show a disordered structure at high and an ordered structure at low temperatures.[13] It is useful to rewrite the Hamiltonian (1) in terms of new variables. Let us introduce new displacements $x_n=\sqrt{B/A}X_n$, temperature (energy scale) $t=TB/AC$, mass

 ©2002 The American Physical Society

$m=MCA^2/\hbar^2B^2$, and a dimensionless parameter $a=A/C$ (we will use $k=1$ and $\hbar=1$ units). Now, the Hamiltonian (1) can be written as

$$h=-\sum_n \frac{\nabla_n^2}{2m}+v,$$

$$v=\left(2d-\frac{a}{2}\right)\sum_n x_n^2+\frac{a}{4}\sum_n x_n^4-\sum_{n,n'} x_n x_{n'}\sigma_{nn'}. \quad (2)$$

A second-order phase transition occurs at certain critical values of temperature and mass, t_c and m_c, respectively. One can easily get all known limits of this model considering the Hamiltonian in the form (2). All four limits of the discrete ϕ^4 model have been extensively studied: order-disorder, displacive, classical, and quantum ones. We briefly review these cases here. A detailed consideration of all limits in the quantum discrete ϕ^4 model is presented in Ref. 14.

The parameter a of the discrete ϕ^4 model determines the type of phase transition in the system and gives two limits: displacive and order-disorder. An order-disorder phase transition takes place at $a\to+\infty$, while a displacive transition occurs at $a\to+0$. These limits correspond to physically different situations, which can be described by well-known models.

The order-disorder limit ($a\to+\infty$) in the classical case ($m\to+\infty$) corresponds to the usual Ising model, and to the Ising model in a transverse field in the quantum case (at finite mass). The order-disorder limit of the discrete ϕ^4 model corresponds to the situation whereby particles can occupy only two positions ($x_n\approx\pm1$). This is the usual classical Ising model in the classical limit ($m\to+\infty$), which has been widely investigated because it is a suitable description of ferromagnetic systems. On the other hand, the system can be imagined as a set of two-level systems with harmonic interaction in an external field in the presence of quantum fluctuations due to strong anharmonicity of the double-well potential. The magnitude of the transverse field implicitly depends on the mass of particles m of the discrete ϕ^4 model. The transverse-field Ising model has been studied for zero and finite temperatures by numerical and various analytical schemes.[15–17]

The displacive limit of the discrete ϕ^4 model ($a\to+0$) is connected to a soft-mode type of phase transition. The system can be presented as a set of uncoupled elementary excitations (phonon vibrations), since the double-well potential becomes almost harmonic. The independent-mode approximation is the convenient method of investigation in this case. The Landau theory also can be used for the description of this limit. The displacive limit in classical and quantum cases has been studied in various applications for real materials,[8–10] because simple experimental methods may reveal soft modes. We mention here two recent works closely related to the considered problem.[18,19] The displacive limit is also extensively studied in the framework of the continuum ϕ^4 model, which is the continuum analog of the discrete one.[20] Both displacive and order-disorder limits for the quantum case are also considered in Ref. 21 in the mean-field approximation.

The classical limit occurs for $m\to+\infty$. Then only thermal fluctuations are present at finite temperature t. The kinetic and potential terms of the partition function can be integrated independently in this case and final results do not depend on the mass of particles. The discrete ϕ^4 model in the classical case has been widely studied by numerical methods and various analytical approaches. The crossover between displacive and order-disorder limits in the frame of this model was discussed by Aubry[12] and later by Padlewski *et al.*[22] A molecular-dynamics study of structural phase transitions is presented in Refs. 23 and 24. The phase diagram for a 2D lattice was obtained by Toral and Chakrabarti.[25] The dynamical character was studied by Flach and Mutschke.[26] Mode-coupling theory was developed for the ϕ^4 lattice model in Refs. 27 and 28. Recently we studied the discrete ϕ^4 model in a 3D classical system[29] and the crossover between 2D and 3D systems.[30]

The pure quantum limit takes place at $t=0$ and the magnitude of the zero-quantum fluctuations is governed by the inverse mass m^{-1}. The quantum fluctuation influence in the framework of the discrete ϕ^4 model is studied in the pure quantum limit ($t=0$) for a wide range of transitions by numerical calculations and analytical approximations.[31] The dependencies of the critical mass m_c on the parameter a for 2D and 3D cases are presented in Figs. 1 and 2 (crosses and lines are numerical and mean-field calculations, respectively). It is expected that a finite temperature will strongly affect the behavior of this system.

Summarizing, the discrete ϕ^4 model has been well studied in the four limits (displacive, order-disorder, classical, or quantum). However, to our knowledge the discrete ϕ^4 model in the presence of quantum and classical fluctuations has not been studied for the general case and for finite temperatures. This work summarizes results of the study of the quantum discrete ϕ^4 model in a wide rage of parameters of the model.

The main aim of this paper is to obtain the quantitative phase diagrams of the quantum discrete ϕ^4 model for 2D and 3D cases. The quantum Monte Carlo (QMC) technique is used as a numerical method. The numerical results are compared with the mean-field (MFA) and independent-mode (IMA) approximations. In the discussion of the obtained results, we put special attention on the crossover between quantum and classical phase transitions and between displacive and order-disorder transitions.

II. ANALYTICAL APPROACHES

A. Mean-field approximation

The MFA is widely used for the study of various phase transitions in ferroelectric and ferromagnetic materials. It is known that this approach describes qualitatively well a wide class of microscopic models with second-order phase transitions. This is also true for the classical discrete ϕ^4 model.[29,30] Here, we present results for the quantum model.

The interaction between particles $\Sigma_{n,n'}x_nx_{n'}\sigma_{n,n'}$ is replaced by an average field $E_n=\Sigma_{n'}x_{n'}\sigma_{n,n'}$ in the MFA. This field does not depend on n ($E_n=E$) in the framework of the discrete ϕ^4 model. The MFA for quantum systems uses the energy levels of the system as data. Let us stress the

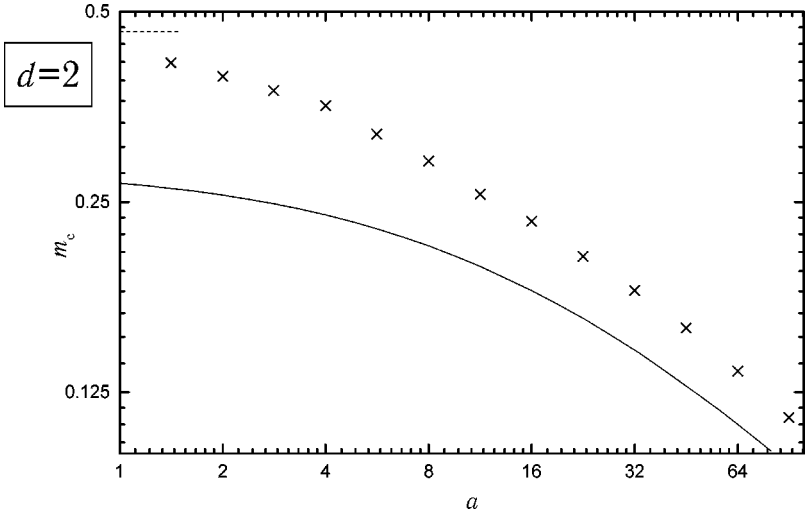

FIG. 1. Dependence of the critical mass m_c on parameter a for the case of $t=0$ in two dimensions. Logarithmic scale is applied for both axes. Crosses: QMC data, obtained by scheme (25) and (27). Solid line: the MFA result. Dashed line: the IMA result.

features of the spectrum of the quantum discrete ϕ^4 model in different limits. We consider the spectrum of the so-called on-site oscillator,

$$H_0=\frac{P^2}{2M}+V_0,$$

$$V_0=\left(2dC-\frac{A}{2}\right)x^2+\frac{B}{4}x^4. \tag{3}$$

There is no interaction between atoms in the Hamiltonian (3). The spectrum of the Hamiltonian (3) is almost equidistant at $a\to+0$ (the system is almost a harmonic oscillator). However, doublets appear in the spectrum of the system at $a\to+\infty$ due to the anharmonicity of the on-site potential V_0 (the spectrum looks like the spectrum of the transverse-field Ising system).

The average of the ground state is proportional to the average field in the MFA and goes to zero at the point of the phase transition. The phase transition takes place at critical values of the mass and temperature (m_c and t_c). It is convenient to rewrite the condition for the phase transition in the MFA for the quantum case as follows:

$$4dC\chi_1=1, \tag{4}$$

where $\chi_1=\partial\langle x\rangle/\partial E$ is the static linear susceptibility, which is determined at a finite temperature by the standard quantum-mechanical formula

$$\chi_1=\sum_{ij}\frac{2d_{ij}^2}{E_i-E_j}\exp\frac{F-E_i}{T}. \tag{5}$$

Here, E_i, d_{ij} are the energy and dipole matrix elements of the Hamiltonian (3), respectively, and F is the free energy. The formula (5) passes into $\chi_1=\Sigma_i 2d_{i0}^2/(E_i-E_0)$ for zero temperature. The energies and matrix elements in Eq. (5) are determined by numerical solution of the Schrödinger equation of the on-site potential (3). The parameters of this problem are the mass m, the temperature t, the model parameter a, and the dimensionality d. The details of these calculations can be found in Ref. 14. The results of calculations in the framework of the MFA are shown in Figs. 1–4. The dependencies of the critical mass m_c on the critical temperature t_c are presented in Figs. 3 and 4 by solid lines for several values of the parameter a ($a=4$, $a=16$, and $a=64$). All curves have an asymptote for the quantum limit ($t=0$; Fig. 1 and 2) and for the classical limit ($m\to+\infty$), which coincides with

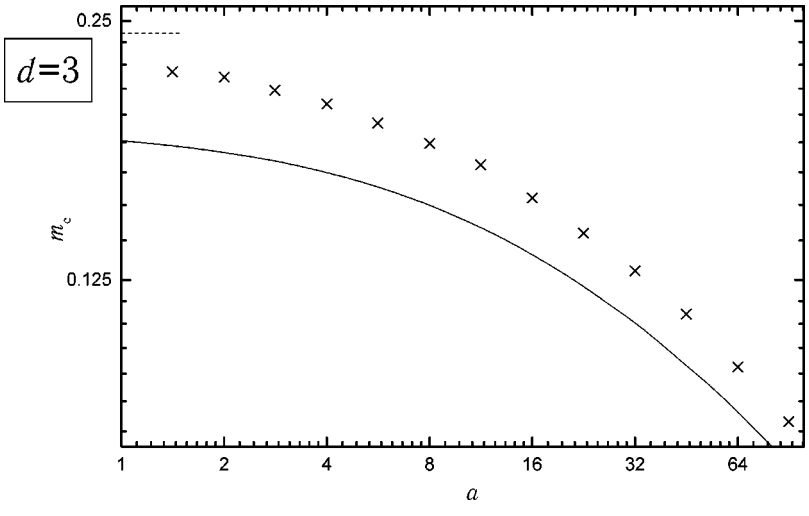

FIG. 2. Dependence of the critical mass m_c on parameter a for the case of $t=0$ in three dimensions. Logarithmic scale is applied for both axes. Crosses: QMC data, obtained by scheme (25) and (27). Solid line: the MFA result. Dashed line: the IMA result.

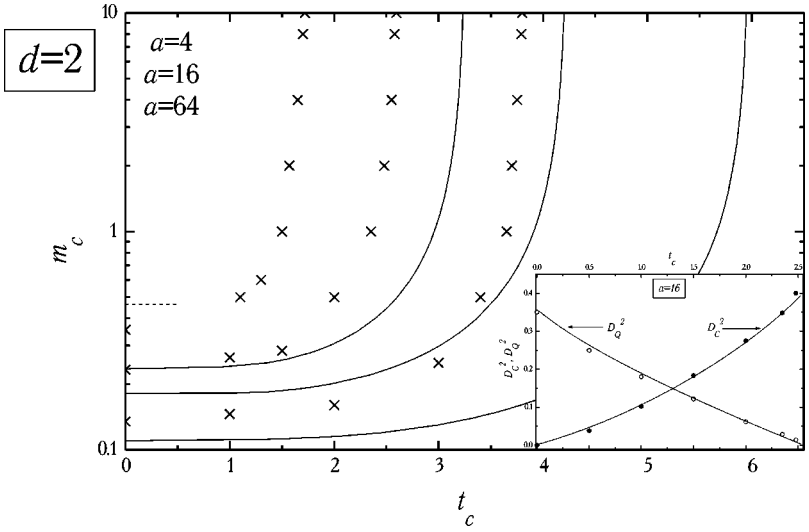

FIG. 3. Phase diagram of the quantum discrete ϕ^4 model for the 2D case: dependencies of the critical mass m_c on the critical temperature t_c (the ordered phase is above and the disordered phase is below it). Crosses: QMC data, solid lines: MFA results, and dashed line: IMA limit in two dimensions ($t=0$, $m_c=0.4649$). QMC and MFA data are presented for three values of the parameter a (from left to right: $a=4$,$a=16$,$a=64$). QMC data at finite temperatures are obtained by schemes (16) and (17) and (16), (17), and (21); data for zero temperature are taken from Fig. 1. Logarithmic scale is used for vertical axis. Inset: the dependence of the "classical" (D_C^2, filled circles) and "quantum" (D_Q^2, opened circles) contributions to fluctuations on the critical temperature t_c for $a=16$ in the 2D case. Lines are guide to the eye.

the results obtained in our previous work with pure quantum and classical discrete ϕ^4 models.[29–31]

B. Independent-mode approximation

The IMA is one of the simplest analytical approaches, used for description of the soft modes in ferroelectric materials.[18,19] This approximation is valid for the case of $a \to +0$ in the classical discrete ϕ^4 model.[13] We generalize this method for the quantum case. The spectrum of the Hamiltonian is almost equidistant and one may consider the system to be a set of the uncoupled harmonic oscillators. One can make a Fourier transform $Q(q)=N^{-1/2}\Sigma_n x_n e^{iqn}$. Then we put $\Sigma Q(q)Q(q_1)Q(q_2)Q(q_3)=3\Sigma Q(q)Q(-q)\Sigma Q(q_1)Q(-q_1)$ (see Ref. 13). The Hamiltonian in the framework of the IMA becomes

$$H_{IMA}=\sum_q \left(\frac{P(q)P(-q)}{2m}+\omega^2(q)Q(q)Q(-q)\right). \quad (6)$$

Here, $Q(q)$ and $P(q)$ are the Fourier transforms of the displacements and momenta of particles, q is a wave vector, and $\omega(q)$ is the dispersion law. The dispersion law of the system can be expressed as

$$\omega^2(q)=-1+4dF(q)+3(I+\eta^2), \quad (7)$$

where $F(q)=1-(1/d)\Sigma_{i=1}^{d}\cos(q_i)$, $I=\langle Q(q)Q(-q)\rangle$, and η is the order parameter. The difference between the classical and quantum cases is in different expressions of the square of the displacement average in the Fourier representation (all other necessary equations of the IMA are the same as those for the classical case).[13] The average I in the classical case can be written as

$$I=\sum_q \frac{t}{\omega^2(q)}, \quad (8)$$

while in the quantum case it should be rewritten as (see Ref. 32)

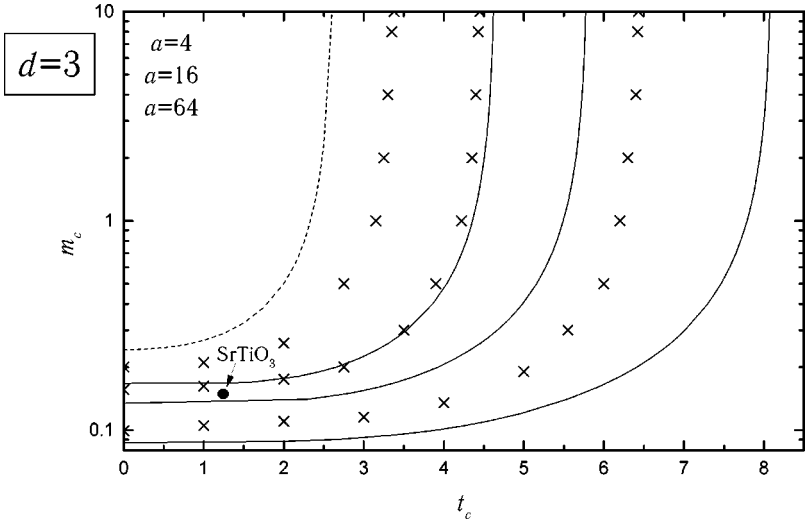

FIG. 4. Phase diagram of the quantum discrete ϕ^4 model for the 3D case: dependencies of the critical mass m_c on the critical temperature t_c (the ordered phase is above and the disordered phase is below it). Crosses: QMC data, solid lines: MFA results, and dashed line: IMA result. QMC and MFA data are presented for the same values of the parameter a as in Fig. 3. QMC data at finite temperatures are obtained by schemes (16) and (17) and (16), (17), and (21); data for zero temperature are taken from Fig. 2. Logarithmic scale is used for vertical axis. The point for $SrTiO_3$ on the phase diagram is placed under the IMA curve, i.e., in the disordered phase (see text for details of estimations).

$$I=\sum_q \left[2\omega(q)\sqrt{m}\tanh\left(\frac{\omega(q)}{2t\sqrt{m}}\right)\right]^{-1}. \quad (9)$$

The equation determining the phase transition is

$$\eta^3+(3I-1)\eta=0. \quad (10)$$

Finally, one can obtain a equation for a critical line $[m_c(t_c)]$ from Eqs. (9), (7), and (10) as follows:

$$\frac{4}{3}=\sum_q \left[\sqrt{m_c dF(q)}\tanh\left(\frac{\sqrt{dF(q)}}{t_c\sqrt{m_c}}\right)\right]^{-1}. \quad (11)$$

The phase-transition line in the 3D case is a smooth curve with well-known asymptotes for the classical ($m\to+\infty$, $t_c=2.638$) and quantum ($t=0$, $m_c=0.2416$) limits (Figs. 2 and 4, dashed lines).[13,31] The phase diagram in the 2D case has only one point at $t=0$ ($m_c=0.4649$; Figs. 1 and 3, dashed lines) due to the divergence of the integral in Eq. (11). It should be pointed out that the classical IMA works at $d\geqslant 3$.[13] The existence of the solution of Eq. (11) in the 2D case in a single point can be bound up with the physical equivalence of the d-dimensional quantum system and the $(d+1)$-dimensional classical one at $t=0$.[33]

III. QUANTUM MONTE CARLO TECHNIQUE FOR THE QUANTUM DISCRETE ϕ^4 MODEL

The QMC technique is used for the numerical study of phase transitions in Bose and Fermi many-body systems with quantum fluctuations.[34,35] The quantum phase transitions are usually divided into transitions at $T=0$ and $T\neq 0$ due to different behavior and classical analogs of the systems.[33] We consider a quantum discrete ϕ^4 model at zero and finite temperatures (and for finite masses) and develop a numerical scheme for these cases. Thus, we present a study of the pure quantum limit and a study of the crossover between quantum and classical limits. The QMC technique used here is based on the Feynman path-integral representation of the partition function.[36] This representation allows to consider a system with quantum fluctuations by reducing to a classical system with other characteristics depending on the Planck constant $\hbar$.

The partition function of the quantum system in the general case is expressed as

$$Z=\mathrm{Tr}(\exp(-H/kT)). \quad (12)$$

In the Feynman path-integral representation the partition function for finite temperature is written as follows:[36]

$$Z=\int [\mathcal{D}x]\exp\left(\hbar^{-1}\int_{-\beta\hbar/2}^{\beta\hbar/2} L(x(\tau))d\tau\right), \quad (13)$$

where $\beta=1/kT$ (in the pure quantum limit $kT=0$, the limits of integration are infinity), $\int[\mathcal{D}x]$ is an integration over the set of all trajectories $x(\tau)$, and $L(x(\tau))$ is the Lagrangian along the imaginary-time trajectory $x(\tau)$. The Lagrangian in our case is

$$L(x(\tau))=-\frac{M}{2}\left(\frac{dx}{d\tau}\right)^2-V(x(\tau)). \quad (14)$$

Note that the negative sign before the kinetic term appears because of the integration along the imaginary-time trajectory $x(\tau)$. Thus, one can conclude by comparison of Eqs. (12) and (13) that a quantum system of dimensionality d with a partition function (13) can be replaced by a classical system of dimensionality $d+1$ (the extra dimension is the imaginary time) at a temperature equal to 1 (see details in Ref. 33; classical $d+1$ systems at $T=0$ and $T\neq 0$ are different). The system is continuous in the extra-time direction, but we need a discrete structure for realization of the Monte Carlo simulations. Discretization of the time direction in the space of the Fourier images appears to be convenient for finite temperatures. However, it is suitable to realize Monte Carlo simulations at zero temperature in real space, since otherwise very long periods of time are needed for averaging. The next two sections are devoted to obtaining the discrete formulas, needed for realization of QMC calculations and discussion of the obtained results for nonzero temperature (first section) and for the pure quantum limit, zero temperature (second section).

A. Discrete scheme for nonzero temperature: Fourier space representation

We develop a discrete scheme for nonzero temperature, which can go into the usual classical Monte Carlo scheme[29,30] in one of its limits. The main idea is to rewrite the integral under the exponent in Eq. (13) in terms of Fourier images and make numerical calculations in Fourier space. This idea was used in Ref. 37 for a Fourier path-integral Monte Carlo method, which has a number of advantageous features. The minor difference with our algorithm is the way we take into account higher harmonics. A single Gaussian random process was used in Ref. 37 for it, while we undertake here the expansion of the Lagrangian in powers of higher harmonics (see below).

The trajectories $x(\tau)$ in Eq. (13) are periodic with period $\beta\hbar$. We make a Fourier transform according to

$$x(\tau)=\sum_{k=-\infty}^{+\infty} x(k)\exp(2\pi ik\tau/\beta\hbar),$$

$$x(k)=\frac{1}{\beta\hbar}\int_{-\beta\hbar/2}^{\beta\hbar/2} x(\tau)\exp(-2\pi ik\tau/\beta\hbar)d\tau, \quad (15)$$

where k is the number of the harmonic. The kinetic term is transformed as (we use here again reduced units t,m, and a; see the Introduction)

$$T=\frac{M}{2}\int_{-\beta\hbar/2}^{\beta\hbar/2}(x'(\tau))^2 d\tau=2\pi^2 mt\sum_{k=-\infty}^{+\infty} k^2 x(k)\overline{x(k)}. \quad (16)$$

The potential energy of the discrete ϕ^4 model after Fourier transformation is

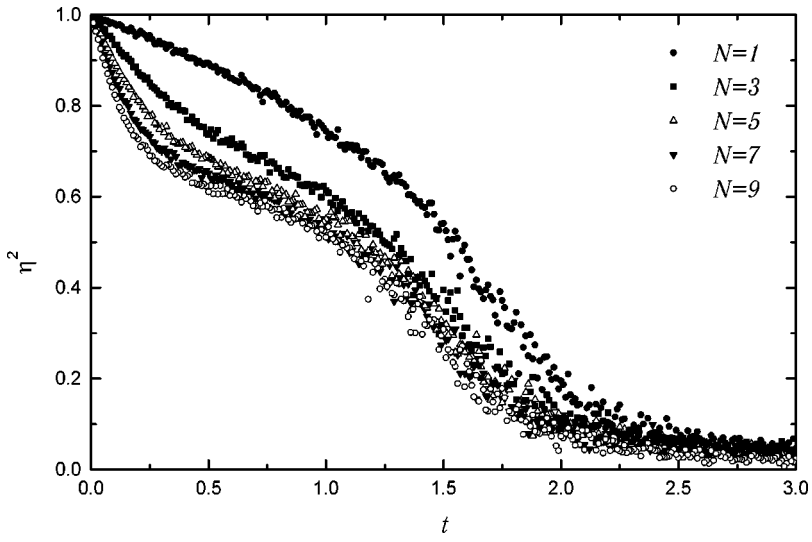

FIG. 5. Dependencies of the square of the order parameter η^2 on the temperature t for different number of harmonics N in the 2D system: QMC data obtained using discrete scheme (16) and (17). Parameter of the model $a=4$, mass of particles $m=1$, and number of harmonics N is varied from 1 to 9 and shown by various symbols. The case $N=1$ corresponds to the classical system.

$$V=\int_{-\beta\hbar/2}^{\beta\hbar/2} V(x(\tau))d\tau$$

$$=\left(2d-\frac{a}{2}\right)\frac{1}{t}\sum_{k=-\infty;n}^{+\infty} x_n(k)\overline{x_n(k)}$$

$$+\frac{a}{4t}\sum_{k,k',k''=-\infty;n}^{+\infty} x_n(k)x_n(k')\overline{x_n(k'')}\,\overline{x_n(k+k'-k'')}$$

$$-\frac{1}{t}\sum_{k=-\infty;n,n'}^{+\infty} x_n(k)\overline{x_{n'}(k)}\sigma_{nn'}. \qquad (17)$$

The displacement $x(k)$ is related to $x(-k)$, since the relation $x(k)=\overline{x}(-k)$ holds. Only a finite number of harmonics is taken into account in the numerical calculations. Thus, we investigate the behavior of the system as a function of the number of harmonics $N=1+2k_{max}$, where k_{max} is the maximum value of k in the sums in Eqs. (16) and (17). Obviously, this scheme goes into the classical one,[29,30] when only one harmonic ($k_{max}=0, N=1$) is taken into account. The other harmonics lead to the appearance of the quantum features in the system. The real quantum system at nonzero temperature is modeled by Eqs. (16) and (17), when an infinite number of harmonics $N\to\infty$ is taken into account.

The typical size of the lattice in QMC calculations for 2D systems is $15\times15\times N$ and $10\times10\times10\times N$ for 3D systems, where N is the size of the extra direction. The periodic boundary conditions in real space are taken into account automatically in the Fourier transform in this scheme. The number of averages is approximately 10^4 per atom. The Metropolis algorithm is used for Monte Carlo sampling.[38] The dependencies of the square of the order parameter on the temperature for a 2D quantum discrete ϕ^4 model at certain parameters ($a=4, m=1$) for a different number of harmonics (varied from $N=1$ to $N=9$) are presented in Fig. 5. The square of the order parameter is calculated as $\eta^2=\langle[N^{*-1}\Sigma_i x_i(0)]^2-[N^{*-1}\Sigma_i x_{i,1}(0)]^2\rangle$ (N^* is the total number of particles).

The last term is a Fourier transform of $x(\tau)$ in x,y directions for the 2D system (in x,y,z directions for the 3D system). It is introduced to reduce the finite-size effects in the calculation.[29] In the numerical calculations with a finite slab, the phase transition is diffused because of strong fluctuations in $\langle x\rangle$ near the transition point. It is natural to suppose that the first and zeroth spatial harmonics of x fluctuate similarly. Therefore, the subtraction of $\langle[N^{*-1}\Sigma_i x_{i,1}(0)]^2\rangle$ should decrease fluctuation. This makes curves more regular and simplifies their analysis. At the same time, below the transition point the correction goes to zero and does not affect the obtained result.

Figure 5 shows that dependencies converge quickly with the increase in the number of harmonics N. However, one needs a large number of harmonics for the description of the behavior of the system at low temperatures, while a few harmonics are sufficient at high temperatures (for example, the curves in Fig. 5 with $N=7$ and $N=9$ harmonics do not differ from each other at $t>0.5$). Nevertheless, the presented curves allow us to determine a temperature of the phase transition for a given number of harmonics.

We use the hypothesis of universality of the discrete ϕ^4 model for the value of the critical index β: $\beta=1/8$ for 2D systems and $\beta\approx0.32$ for 3D systems at any value of the parameter a (there is the exclusion in the point $a=0$: here the Landau theory is valid and $\beta=1/2$).[13] For example, we present the dependence of the $\eta^8(t)$ for a 2D system with $N=9$ harmonics [Fig. 6(a)]. The solid line is the approximation by the linear dependence. The temperature of the phase transition t_c obtained in this way does not change when increasing the size of the system. This method of determination of the temperature of the phase transition shows the same temperature in the classical limit ($N=1$) as the one obtained in Ref. 30 for classical systems in another way (at the point of the minimum of the first derivative). The temperature of the phase transition t_c as a function of the number of harmonics N, extracted from data in Fig. 5, is represented in Fig. 6(b) by the open symbols.

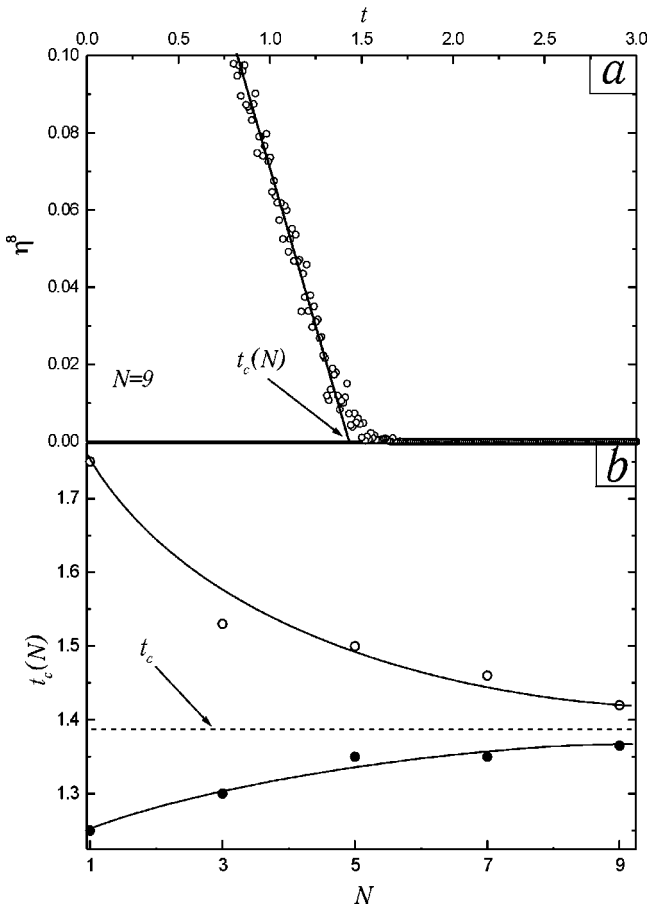

FIG. 6. Determination of the temperature of the phase transition in the quantum discrete ϕ^4 model from QMC data. (a) Circles: dependence of the η^8 on the temperature t for the 2D system at $N=9$, $a=4$, and $m=1$ [dependence $\eta^2(t)$ is shown in Fig. 5]. The power of the order parameter is taken from the value of the critical indices of the model (see text). Solid line is a linear approximation of the QMC data. Arrow shows critical temperature t_c. (b) Critical temperature t_c as a function of the number of harmonics N with the same parameters of the model. Open symbols: result obtained using discrete scheme (16) and (17). Filled symbols: result obtained using discrete scheme (16), (17), and (21), where the influence of higher harmonics is taken into account. Solid lines: guide to the eye. These curves converge to the real t_c (infinite N) of the model at given parameters m,a (dashed line).

To develop a better accuracy for a small number of Fourier components a higher-order numerical scheme is needed. Data presented in Fig. 5 are not sufficient for determination of the real temperature of the phase transition of the system, since it is impossible to make numerical simulations with all harmonics. To determine the sought temperature of the phase transition one can use the following method, which allows us to take into account the influence of all the other harmonics. Let us divide $x(\tau)$ in Eq. (15) into two parts $x_0(\tau)$ (slow) and $x_f(\tau)$ (fast), where the first one takes into account N harmonics (from $-k_{max}$ to k_{max}) and the second one includes all the other harmonics:

$$x(\tau)=x_0(\tau)+x_f(\tau)=\sum_{|k|\leqslant k_{max}} x(k)\exp(2\pi ik\tau t) + \sum_{|k|>k_{max}} x(k)\exp(2\pi ik\tau t). \tag{18}$$

Next, one can make a Taylor expansion of $L(x(\tau))$ in Eq. (13) in powers of $x_f(\tau)$ keeping the terms up to the $x_f^2(\tau)$. One can check that the coefficients of this expansion are adiabatically slowly varying functions. The partition function after these transformations can be rewritten as

$$Z=\int [\mathcal{D}x_0]\exp\left(-\int_{-\infty}^{+\infty} L(x_0(\tau))d\tau\right) \times \int [\mathcal{D}x_f]\exp\left(-\sum_{|k|>k_{max}} (2m\pi^2k^2+V'')x_f^2(k)\right). \tag{19}$$

One can integrate the fast part of the partition function (19) or use the method for calculation of this type of integral, described in Ref. 36. This part turns out to be proportional to

$$\exp\left(-\frac{1}{2}\sum_{|k|>k_{max}} \frac{V''}{4mt^2\pi^2k^2}\right). \tag{20}$$

We write a correction, with integrated harmonics, for the discrete scheme (16) and (17) as a function of N:

$$\frac{V''\xi(N)}{mt^2}, \tag{21}$$

where the numerical coefficients are $\xi(1)=\frac{1}{24}$, $\xi(3)=\frac{1}{24}-1/4\pi^2$, $\xi(5)=\frac{1}{24}-5/16\pi^2$, $\xi(7)=\frac{1}{24}-49/144\pi^2$, $\xi(9)=\frac{1}{24}-205/576\pi^2$. Thus, we take into account the effective influence of high harmonics by their integration and by adding a term (21) to the discrete formula (16) and (17). At $N=1$ the formula (21) coincides with the quantum correction obtained in Ref. 36.

Now we come to the finite temperature, obtained by scheme (16) and (17) for N harmonics with correction (21) for the influence of all other harmonics. First of all, we note that the scheme does not work at low temperatures with a small number of harmonics due to divergency. The dependencies of the square of the order parameter on the temperature for $m=2$ and for $m=0.5$ for various N obtained using scheme (16), (17), and (21) are presented in Figs. 7 and 8, respectively. One can see from these dependencies that at high masses (for example, $m=2$, Fig. 7) even a single harmonic ($N=1$) is sufficient determine the temperature of the phase transition at a given mass. On the other hand, we need more than one harmonic for low masses and temperatures for determining the transition temperature (for example, $m=0.5$, Fig. 8). Obviously, the real dependence of the square

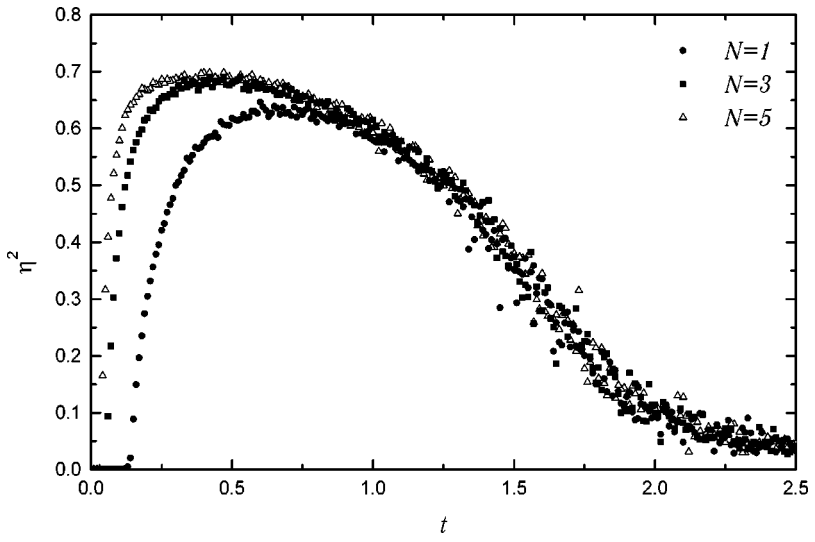

FIG. 7. Dependencies of the square of the order parameter η^2 on the temperature t for different number of harmonics N in the 2D system: QMC data obtained using discrete scheme (16), (17), and (21), which includes influence of higher harmonics. Parameters of the model: $m=2$, $a=4$. Small N is sufficient for determination of the $t_c(N)$, which is used for determination of the t_c [Fig. 6(b)].

of the order parameter on the temperature at given m and given N is placed between two curves: obtained by scheme (16) and (17) and scheme (16), (17), and (21). The real transition temperature is also between the two curves: temperatures of the transition as a function N obtained using schemes (16) and (17) are given by open symbols and for (16), (17), and (21) by filled symbols [Fig. 6(b)]. Two curves in Fig. 6(b) converge to the true transition temperature of the model. Normally, a number of harmonics $N=5$ is sufficient to determine the critical values (m_c, t_c) with accuracy about 2% at $t>1.5$.

We plot a phase diagram of the quantum discrete ϕ^4 model determining the critical temperatures t_c and masses m_c as shown in Fig. 6(b) for certain parameters of the model. The phase diagrams (dependencies of m_c on t_c) for 2D and 3D systems at various values of the parameter a ($a=4$, $a=16$, and $a=64$) of the quantum discrete ϕ^4 model are presented in Figs. 3 and 4. The $N=7$ or $N=9$ are used for obtaining the critical values (m_c, t_c). We estimate the accuracy of the determination of the critical temperature to be better than 1% for $m>2$ and about 2% for smaller masses. Obviously, the accuracy can be increased by increasing the number of harmonics N in QMC calculations.

B. Discrete scheme for the pure quantum limit: real-space representation

The discrete scheme obtained in the previous section cannot be used for the case of the pure quantum limit ($t=0$), since one needs to take into account an infinite number of harmonics at $t=0$. To avoid this kind of difficulty one can make the inverse Fourier transform of all formulas obtained above and fulfill the Monte Carlo averaging in the real space of displacements.

The main difference with the case of finite temperature appears in the unlimited integration limits in Eq. (13). To obtain the discrete formula for this case one can take the following step. Let the value $\beta\hbar$ go to infinity, taking into account a finite number of harmonics. Then, the series in Eq. (15) goes into an integral and the value $\omega=1/2\tau_0$ in the integral appears instead of k_{max} in the sum (18) (τ_0 is the discrete step in the extra-time direction; τ_0 can be considered an analog of N in finite-temperature calculations). Now, the formula (16) becomes

$$T=\frac{M}{2}\int_{-\infty}^{+\infty}(x'(\tau))^2 d\tau = 2\pi^2 m\int_{-1/2\tau_0}^{+1/2\tau_0}\epsilon(\omega)x_0^2(\omega)d\omega, \tag{22}$$

where $\epsilon(\omega)=\omega^2$ is the dispersion law. Thus, we have after inverse Fourier transform (the discretization is carried out as $\int dt\to\tau_0\Sigma_i i$)

$$T=2\pi^2 m\tau_0^2\sum_{i,j,k;i+j+k=0}\epsilon(i\tau_0)x_0(j\tau_0)x_0(k\tau_0). \tag{23}$$

The dispersion law is transformed as

$$\epsilon(\tau)=\int_{-1/2\tau_0}^{1/2\tau_0}\omega^2\exp(i2\pi\omega\tau)d\omega=\frac{(-1)^i}{2i^2\pi^2\tau_0^3}\quad \tau\neq 0, \tag{24}$$

$$\epsilon(0)=\frac{1}{12\tau_0^3}\quad \tau=0.$$

Finally, the discrete formula for the integral under the exponent in Eq. (13) is as follows:

$$\frac{m}{\tau_0}\sum_{i,j,k;i+j+k=0}\frac{(-1)^i}{i^2}x_0(j\tau_0)x_0(k\tau_0)+\frac{\pi^2 m}{6\tau_0}\sum_i x_0^2(i\tau_0) + \tau_0\sum_i V(x_0(i\tau_0)). \tag{25}$$

To take into account higher harmonics we use the same method as in the case of nonzero temperature. The sum in the

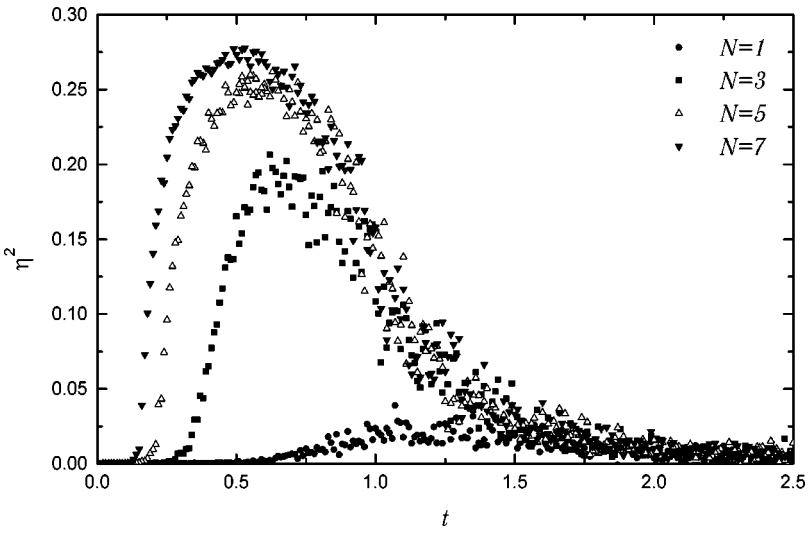

FIG. 8. Dependencies of the square of the order parameter η^2 on the temperature t for different number of harmonics N in the 2D system: QMC data obtained using discrete scheme (16), (17), and (21), which includes influence of higher harmonics. Parameters of the model: $m=0.5$, $a=4$. One needs more harmonics at low masses for determination of the temperature of the phase transition, than at higher masses (see Fig. 7).

fast part of the partition function (19) goes into the integral $\int_{|\omega|>1/2\tau_0} d\omega$. Now, the fast part of the partition function is proportional to

$$\exp\left(-\frac{\tau_0}{2} \int_{|\omega|>1/2\tau_0} \frac{V''}{4m\pi^2\omega^2} d\omega \right). \tag{26}$$

Therefore, one should add to the discrete formula (25) the following correction, which includes the influence of the higher harmonics:

$$\frac{\tau_0^2}{2\pi^2 m} \sum_i V''(x_0(i\tau_0)). \tag{27}$$

The discrete scheme (25) and (27) for zero temperature converges as τ_0^2. Periodic boundary conditions should be applied in the extra-time dimension, since the Feynman trajectories are closed in real space. The typical size of the lattice in the Monte Carlo simulations is $10^d \times 100$, at 10^4 averaging per atom. The value of τ_0 is approximately equal to 0.1, which is sufficient for the determination of the critical masses m_c with accuracy 2%. The dependencies of the square of the order parameter on the mass of atoms are obtained for various values of the parameter a. Critical values of masses m_c are extracted from these curves by linear approximation in appropriate coordinates. The results for 2D and 3D systems are presented in Figs. 1 and 2 by crosses. We estimate the error bar to be 2%. These data are also presented in Figs. 3 and 4 for $a=4$, $a=16$, and $a=64$.

IV. DISCUSSION

Let us analyze the results explained above. We have presented phase diagrams for finite temperature (Figs. 3 and 4) and for zero temperature (Figs. 1 and 2) in 2D and 3D cases obtained by numerical methods (QMC) and by analytical approaches (MFA and IMA). The ordered phase is above the critical line [$m_c(t_c)$ in Figs. 3 and 4 or $m_c(a)$ in Figs. 1 and 2], while the disordered one is below it.

The results for finite temperature in the 2D and 3D cases obtained by QMC for three values of the parameter a ($a=4, a=16, a=64$) of the considered model are shown in Figs. 3 and 4 by crosses, respectively. The analytical study of the finite-temperature case is presented by solid lines (MFA) (for the same three parameters a) and dashed lines (IMA). Note that the IMA results do not depend on the value of the parameter a and correspond to the displacive limit $a \to +0$ (the IMA works in the 2D case only for zero temperature, Figs. 1 and 3). All results (QMC, MFA, IMA in three dimensions and QMC, MFA in two dimensions) show in the classical limit $m \to +\infty$ quantitative agreement with our previous studies of the classical model[29,30] obtained by classical analogs of the same methods. For the purely quantum limit, the results of finite-temperature calculations tend to the zero-temperature ones. Thus, the finite-temperature scheme works well for all points of the phase diagram. Note that to increase the accuracy of the QMC results at low temperatures or to obtain $t=0$ limits one should increase the number of harmonics in the QMC scheme in Fourier space (finite-temperature algorithm). However, this demands large computing resources.

The results for zero temperature in the 2D and 3D cases obtained by QMC for a wide range of the parameter a of the quantum discrete ϕ^4 model are shown in Figs. 1 and 2 by crosses, respectively. The analytical study at zero temperature is presented by solid lines (MFA) and dashed lines (IMA). Note the IMA in the pure quantum limit works in both cases (2D and 3D), but still only in $a \to +0$. The QMC, MFA, and IMA results at $t=0$ can be used as asymptotes (i.e., the pure quantum limit) for the finite-temperature results at low temperatures (zero-temperature results are also presented in Figs. 3 and 4 for $a=4, a=16, a=64$).

The general analysis of the obtained results shows a good qualitative agreement between the MFA and QMC results in a wide range of parameters of the quantum discrete ϕ^4 model. This confirms that the MFA is a suitable approach for the study of the qualitative behavior of the systems not only in the classical case but also in the presence of quantum fluctuations. The MFA overestimates QMC finite-temperature results by 90% for $a=4$ and by 60% for a

$=16$, $a=64$ at $m \gtrsim 1$ in the 2D case (Fig. 3). The error bar at $m \lesssim 1$ becomes larger in the temperature scale. Overestimation for the 3D finite-temperature case (Fig. 4) is smaller than in the 2D case and comes to 40% for $a=4$ and less than 30% for $a=16$, $a=64$ at $m \gtrsim 0.5$ (it becomes larger at $m \lesssim 0.5$). The MFA results underestimate QMC zero-temperature ones by 50% for small values of $a (a \lesssim 8)$ and by less than 30% for large values of $a (a \gtrsim 8)$ in the 2D case (Fig. 1). The error bar is decreased in the 3D case (Fig. 2): 20% for $a \lesssim 8$ and less than 15% for $a \gtrsim 8$.

The IMA approach can be used to study the displacive limit, since QMC curves tend to IMA results as a goes to zero. We believe QMC results reproduce IMA ones at $a \to +0$ in the 2D case for $t=0$ and in the 3D case for all temperatures.

The presented results demonstrate a crossover between the quantum ($t=0$) and classical ($m \to +\infty$) limits. As was discussed, the nature of fluctuations is different for the two limits. Here we estimate quantum and thermal contributions to fluctuations quantitatively. As a measure of thermal fluctuations, the value of $D_C^2 = \langle N^{*-1} \Sigma_i [\overline{x} - x_i(0)]^2 \rangle$ is used. This is a dispersion of the zeroth imaginary-time Fourier harmonic. In the classical limit all other harmonics are absent, and D_C^2 determines the dispersion of x. For the quantum limit D_C^2 vanishes. The quantum fluctuations are determined from other harmonics: $D_Q^2 = \langle N^{*-1} \Sigma_{i,k;k \neq 0} [x_i(k)]^2 \rangle$. The comparison of these two quantities allows us to make judgements about the main type of fluctuations presented in the system and in that way to describe the crossover between quantum and classical limits. For instance, the results for the 2D case and $a=16$ are presented in the inset to Fig. 3. For each value of temperature, the corresponding critical value of the mass is used, so that all points in this inset are calculated for the critical line in the phase diagram. This inset shows that at low temperature the influence of the thermal (classical) fluctuations is decreased, while the influence of the quantum fluctuations is increased. The situation at higher temperature is the inverse. We estimate that the quantum limit occurs at $t < 0.25$, while the classical one takes place at $t > 2.25$. Both types of fluctuations have an influence on the behavior of the system, when the temperature is between these two values.

We also would like to stress that the presented results show a crossover between displacive and order-disorder limits. Displacive behavior is found for $a < 1$ as follows from previous studies.[29,31] As for the order-disorder limit, the value of the parameter a, at which this limit occurs can be estimated, for example, in the framework of the MFA, by comparing the spectrum of the ϕ^4 model with the spectrum of the transverse-field Ising model (see details in Ref. 14). Order-disorder behavior is found for $a > 60$ at moderate masses as seen from MFA calculations. Thus, obtained results cover a wide range of phase transitions in the quantum discrete ϕ^4 model: from displacive to order-disorder types.

The quantum discrete ϕ^4 model is certainly one of the simplest models for the description of materials and does not take into account the complicated structure of real systems. However, it can be used for qualitative estimations of some real quantum paraelectrics. We present here an estimation for $SrTiO_3$. We use the method described in Ref. 14. There is a phase transition at $T \approx 105$ K, which is of the classical type.[13] As is well known, Landau theory predicts another phase transition in $SrTiO_3$ at $T_c \approx 50$ K, which does not exist because it is suppressed by quantum fluctuations.[39] We assume that the oxygen atoms are placed in double-well potentials, formed by the rest of the atomic lattice. The estimations for the parameter a give that this material is in the displacive limit ($a \approx 0.17$).[14] Thus, the IMA is valid and we can use the curve found in this approximation (Fig. 4, dashed line). We use the following relation for an estimation of the mass, $m \approx MkT_c \langle \triangle x^2 \rangle / \hbar^2 \lambda$, where the constant $\lambda = kT_c B/AC = 2.64$ defines the displacive limit and the value $\langle \triangle x^2 \rangle$ is the square of half the distance between two minima of the double-well potential (a recent estimation gives $\langle \triangle x^2 \rangle \approx 0.9 \times 10^{-22}\ m^3$). Finally, we have $m \approx 0.15$. This point ($t \approx 1.25$, $m \approx 0.15$) lies below the IMA curve (Fig. 4, dashed line), i.e., in the disordered phase. This is in agreement with the assumption that the phase transition is suppressed by quantum fluctuations as follows from experimental data.[39] Thus, the quantum discrete ϕ^4 model qualitatively predicts the behavior of $SrTiO_3$. However, the mass difference between O^{16} and O^{18} is not sufficient to shift the point from the disordered phase to the ordered one. Thus this model cannot explain the results of the experiment (see Ref. 2). The reason is that the discrete ϕ^4 model is too simple a model for $SrTiO_3$. The models, used for the description of $SrTiO_3$, are much more complicated[40] and include other couplings between the various atoms.[41–43] Nevertheless, we believe the quantum discrete ϕ^4 model can be used for a qualitative description of ferroelectric materials also for low temperatures and it gives qualitative agreement with experimental observations.[14]

V. CONCLUSIONS

In conclusion, we have studied phase diagrams of the quantum discrete ϕ^4 model in 2D and 3D cases. Two crossovers can be observed in this model: from a displacive to an order-disorder phase transition and from a classical to a quantum phase transition. The first crossover is governed by the parameter a, while the second one is governed by two parameters, m and t (reduced mass and temperature, respectively). The dependencies of the order parameter $\eta(a,m,t)$ and the phase diagram $m_c(a,t_c)$ may be used for the description of some real ferroelectric materials with phase transition of various types, including quantum and thermal fluctuations.

We use the QMC technique for the study of phase diagrams in the frame of the quantum discrete ϕ^4 model. For given parameters a,m or a,t we can determine temperature t_c or mass m_c of the phase transition, respectively. These show crossovers from the displacive to the order-disorder limit and from quantum to classical behavior.

We have obtained two discrete schemes for performing QMC calculations: one in Fourier space (for $t > 0$) and another in real space (for $t=0$). These schemes have been used for obtaining dependencies of the square of the order parameter η^2 in a wide range of the parameters a and m. Critical

values t_c and m_c are extracted from these dependencies. Phase diagrams $[m_c(t_c)]$ at various values of parameter a show good agreement with classical limits taken from our previous studies of this model. Results obtained by Fourier space algorithm tend to results obtained by real-space algorithm as t goes to zero. We estimate the accuracy of QMC calculations to be less than 1% at $m>1$ and a few percent in the quantum area $(m<1)$.

The analytical MFA and IMA have been generalized for the case of two types of fluctuations: quantum and thermal ones. The phase diagrams have been also obtained in the framework of the MFA and shown qualitative agreement with QMC calculations for various values of parameters of the quantum discrete ϕ^4 model. Overestimations or underestimations of the QMC results are varied from tens to hundreds of percent depending on the parameters of the model. IMA results demonstrate quantitative agreement with QMC results for the 3D case and for the 2D case at $t=0$ at small values of a.

Presented data show crossovers from a displacive to an order-disorder phase transition and from a classical to a quantum phase transition. The appearance of the order-disorder limit depends on the mass m. It takes place at $a>60$ at $m\sim 1$, while the displacive limit occurs at $a<1$. Quantum fluctuations start to play an essential role at $t\lesssim 1$ depending on the parameters of the model. The temperature of the phase transition does not differ strongly from the classical one at $m\gtrsim 2$ for 2D and 3D systems.

$SrTiO_3$ has been considered in the framework of the quantum discrete ϕ^4 model. The estimation for $SrTiO_3$ shows a disordered phase of this crystal at $T\approx 50$ K, which coincides with experimental data.

ACKNOWLEDGMENTS

This work was done in the framework of an INTAS project for young scientists (Grant No. YSF 2001/1-135). Also, it was partly supported by the RFFI foundation (Grant No. 00-02-16253, and special grants for young scientists) and by the ''Russian Scientific Schools'' program (Grant No. 96-1596476).

[1] K.A. Müller and H. Burkard, Phys. Rev. B **19**, 3593 (1979).
[2] M. Itoh, R. Wang, Y. Inaguma, T. Yamaguchi, Y-J. Shan, and T. Nakamura, Phys. Rev. Lett. **82**, 3540 (1999).
[3] A. Bussmann-Holder, H. Büttner, and A.R. Bishop, J. Phys.: Condens. Matter **12**, L115 (2000).
[4] O.E. Kvyatkovskii, Phys. Solid State **43**, 1401 (2001).
[5] W. Zhong and D. Vanderbilt, Phys. Rev. B **53**, 5047 (1996).
[6] L. Zhang, W-L. Zhong, and W. Kleemann, Phys. Lett. A **276**, 162 (2000).
[7] W. Zhong, D. Vanderbilt, and K.M. Rabe, Phys. Rev. Lett. **73**, 1861 (1994).
[8] S.A. Prosandeev, W. Kleemann, and J. Dec, Integr. Ferroelectr. **32**, 979 (2001).
[9] S.A. Prosandeev, A.E. Maslennikov, W. Kleemann, and J. Dec, Ferroelectrics **238**, 735 (2000).
[10] S.A. Prosandeev, W. Kleemann, and J. Dec, J. Phys.: Condens. Matter **13**, 5957 (2001).
[11] J. Hlinka, T. Janssen, and V. Dvorak, J. Phys.: Condens. Matter **11**, 3209 (1999).
[12] S. Aubry, J. Chem. Phys. **62**, 3217 (1975).
[13] A. D. Bruce and R. A. Cowley, *Structural Phase Transitions* (Taylor & Francis, London, 1981).
[14] V.V. Savkin and A.N. Rubtsov, cond-mat/0112429 (unpublished).
[15] B. K. Chakrabarti, A. Dutta, and P. Sen, *Quantum Ising Phases and Transitions in Transverse Ising Models, Lecture Notes in Physics* (Springer-Verlag, Heidelberg, 1996), Vol. M41, and references therein.
[16] J.W. Kim, M.L. Ristig, and J.W. Clark, Phys. Rev. B **57**, 56 (1998).
[17] V.Yu. Irkhin and A.A. Katanin, Phys. Rev. B **58**, 5509 (1998).
[18] J.M. Perez-Mato and E.K.H. Salje, J. Phys.: Condens. Matter **12**, L29 (2000).
[19] S.A. Prosandeev, V.A. Trepakov, M.E. Savinov, and S.E. Kapphan, J. Phys.: Condens. Matter **13**, 1 (2001).
[20] V.G. Rostiashvili and R. Schilling, Phys. Rev. Lett. **72**, 2130 (1994).
[21] S.A. Prosandeev, W. Kleemann, B. Westwanski, and J. Dec, Phys. Rev. B **60**, 14 489 (1999).
[22] S. Padlewski, A.K. Evans, and C. Ayling, J. Phys.: Condens. Matter **4**, 4895 (1992).
[23] T. Schneider and E. Stoll, Phys. Rev. B **13**, 1216 (1976).
[24] T. Schneider and E. Stoll, Phys. Rev. B **17**, 1302 (1978).
[25] R. Toral and A. Chakrabarti, Phys. Rev. B **42**, 2445 (1990).
[26] S. Flach and G. Mutschke, Phys. Rev. E **49**, 5018 (1994), and references therein.
[27] S. Flach and J. Siewert, J. Phys.: Condens. Matter **4**, L363 (1992).
[28] S. Flach, J. Siewert, R. Siems, and J. Schreiber, J. Phys.: Condens. Matter **3**, 7061 (1991).
[29] A.N. Rubtsov, J. Hlinka, and T. Janssen, Phys. Rev. E **61**, 126 (2000).
[30] V.V. Savkin and A.N. Rubtsov, Zh. Éksp. Teor. Fiz. **118**, 1391 (2000) [Sov. Phys. JETP **91**, 1204 (2000)].
[31] A.N. Rubtsov and T. Janssen, Phys. Rev. B **63**, 172101 (2001).
[32] L. D. Landau and E. M. Lifshitz, *Statistical Physics* (Pergamon Press, Oxford, 1977).
[33] S.L. Sondhi, S.M. Girvin, J.P. Carini, and D. Shahar, Rev. Mod. Phys. **69**, 315 (1997), and references therein.
[34] D.M. Ceperley, Rev. Mod. Phys. **67**, 279 (1995), and references therein.
[35] W.M.C. Foulkes, L. Mitas, R.J. Needs, and G. Rajagopal, Rev. Mod. Phys. **73**, 33 (2001), and references therein.
[36] R. Feynman and A. R. Hibbs, *Quantum Mechanics and Path Integrals* (McGraw-Hill, New York, 1965).
[37] J.D. Doll, Rob D. Coalson, and David L. Freeman, Phys. Rev. Lett. **55**, 1 (1985), and references therein.
[38] M. H. Kalos and P. A. Whitlock, *Monte Carlo Methods Volume 1:*

Basics (Wiley, New York, 1986).
[39] H.M. Christen, J. Mannhart, E.J. Williams, and Ch. Gerber, Phys. Rev. B **49**, 12 095 (1994).
[40] K.A. Müller, W. Berlinger, and E. Tosatti, Z. Phys. B: Condens. Matter **84**, 277 (1991).
[41] H. Bilz, G. Benedek, and A. Bussmann-Holder, Phys. Rev. B **35**, 4840 (1987).
[42] A. Bussmann-Holder, H. Bilz, and G. Benedek, Phys. Rev. B **39**, 9214 (1989).
[43] A. Bussmann-Holder, Phys. Rev. B **56**, 10 762 (1997).